



Branched silica nanostructures oriented by dynamic G-quadruplex transformation

Jinli Zhang^a, Lin Zheng^a, Xian Wang^a, Ying Xiao^b, Yi Lu^c, Wei Li^{b,*}

^a Key Laboratory of Systems Bioengineering School of Chemical Engineering and Technology, Tianjin University, Tianjin 300072, China

^b Key Laboratory for Green Chemical Technology, Ministry of Education School of Chemical Engineering and Technology, Tianjin University, Tianjin 300072, China

^c Department of Chemistry, University of Illinois at Urbana-Champaign Urbana, IL 61801, USA

ARTICLE INFO

Article history:

Received 1 January 2010

Received in revised form 22 June 2010

Accepted 22 August 2010

Available online 27 August 2010

Keywords:

A. Inorganic compounds

A. Nanostructures

C. Atomic force microscopy

ABSTRACT

Polymorphic G-quadruplexes including stacked G-quartet planes are potentially promising DNA templates beyond Watson–Crick duplexes to construct inorganic nanostructures. In this work, a novel G-rich oligonucleotide that can be modulated from the antiparallel G-quadruplex to multi-stranded supermolecular assemblies was designed. Based on this dynamic G-quadruplex transformation, an interesting leaf-vein silica nanostructure with regular branched intervals was constructed. The G-quadruplex assembly structure was found to play a significant role in the organization of the silica structures.

© 2010 Elsevier Ltd. All rights reserved.

1. Introduction

DNA self-assembly is increasingly recognized as an effective way to construct well-defined nanostructures for directing the organization of inorganic nanomaterials owing to its advantage of programmable molecular recognition [1–6]. Several self-assembled DNA nanopatterns based on the conventional Watson–Crick duplex have been developed to organize the oxide nanoparticles, such as the rod-like and circular silica fibers [7,8], titania nanotubes [9], magnetic nanowires [10], etc. Despite the progresses that have been made, using self-assembled DNA templates to create hybrid nanomaterials with increasingly complicated structures is still a principle challenge; meeting such a challenge will not only enable precise spatial positioning of individual units in nano-fabrication [11] but also promote the development of bioinspired synthesis of novel function materials [12].

One approach to meeting the above challenge is to construct nanostructures using DNA beyond Watson–Crick duplex structures. Guanine (G)-rich oligonucleotides can self-assemble into polymorphic quadruplexes via stacking of G-quartets comprising of eight intermolecular hydrogen bondings (e.g., N2–H...N7, N1–H...O6) between neighboring guanine residues [13–15]. Based on the self-association of G-quadruplexes, a number of G-wire structures involving the linear wire of G₄T₂G₄ [16–18], the frayed

wires of A₁₅G₁₅ [19,20], the G-lego of G₁₁T [21], etc., have been studied due to their advantage in generating unique nanopatterns over DNA duplexes. However, the potential of G-quadruplex in constructing highly ordered oxide nanostructures has not been fully explored.

Herein, we reported a novel asymmetric G-quadruplex G₂T₄G₄ that can be modulated to transform into multi-stranded supermolecular assemblies. Based on this original G-quadruplex transformation, leaf-vein nanostructures of silica with regular branched intervals were organized.

2. Experimental

G-rich DNA oligonucleotides of G₂T₄G₄, G₃T₄G₄ and G₄T₄G₄ were purchased from the Japanese Takara Bio (Dalian) with the purity higher than 98%. Before the experiments, all samples were diluted to a final concentration of 40 μM in a 100 mM NaCl aqueous solution (pH 5.9) or 100 mM KCl as mentioned in the text. The DNA samples were then annealed at 95 °C for 5 min, slowly cooled to 4 °C, and holding at this temperature for several hours. To synthesize DNA-silica hybrid nanoparticles, an ethanol solution of 3-aminopropyl trimethoxysilane (APTMS) (5 μL, 10%, v/v) was added into an aqueous solution of G-rich DNA (400 μL, 40 μM) under stirring, with a molar ratio APTMS/DNA of 179. The mixture was allowed to react at 20 °C for 18 h. The generated DNA-silica nanostructures were characterized by AFM and high-resolution transmission electron microscope (HRTEM). As a control, silica nanoparticles were synthesized under the similar conditions in the absence of DNA.

* Corresponding author. Tel.: +86 22 27890643; fax: +86 22 27890643.
E-mail address: liwei@tju.edu.cn (W. Li).

CD spectra were obtained from a Jasco J-810 spectropolarimeter equipped with a Julabo temperature controller. Thermal denaturation profiles were collected in units of millidegrees as a function of temperature. The heating rate was fixed at $1.0\text{ }^{\circ}\text{C min}^{-1}$. CD stopped-flow kinetic measurements were performed with SFM300 multi-mixing instruments (Bio-logic). Time courses were recorded in units of millidegrees at $20\text{ }^{\circ}\text{C}$ with a sample period of 200 ms at 293 nm upon mixing the aqueous solution of $\text{G}_2\text{T}_4\text{G}_4$ and APTMS-containing ethanol solution at the volume ratio of 9:1. Data sets from at least four experiments performed under identical conditions were averaged and then fitted to a single-exponential equation using Igor software (Wave-Metrics Inc., USA).

Native polyacrylamide gel electrophoresis (PAGE) measurements were carried out to characterize the electrophoresis mobility of DNA structures using 20% acrylamide [29:1 acrylamide/bis(acrylamide)] at 10 V cm^{-1} and $4\text{ }^{\circ}\text{C}$. The gel was stained in a $3\text{ }\mu\text{g mL}^{-1}$ Gelred solution for 30 min. The intensity of each band in the native PAGE images was determined using a GDS8000 system (UVP, Inc., USA).

AFM measurements were carried out under constant repulsive force mode by AFM (AJ-IIIa, Aijian nanotechnology Inc., China). Samples were prepared for measurements by dropping $10\text{ }\mu\text{L}$ solution onto a freshly cleaved mica substrate for 10 min, followed by washing with water and rapidly drying by N_2 . All AFM images were obtained in the tapping mode in air under normal conditions.

SER spectra were measured with a Renishaw MKI-2000 laser confocal microscopy Raman spectrometer with a CCD detector and a holographic notch filter (Renishaw Ltd., Gloucestershire, UK). The spectral resolution for this experiment was 2 cm^{-1} . Radiation of 633 nm from an air-cooled argon ion laser was used for the SER spectra excitation. For SER spectra, citrate-reduced Au nanoparticles (with an average diameter of 42 nm), prepared by a standard protocol [22], were added into the DNA solution with equal

volume. $20\text{ }\mu\text{L}$ volume of the sample was deposited in a depression slide and the spectra were recorded.

The zeta potential of the silica particles in solution formed by APTMS hydrolysis was determined using a Zeta Plus zeta potential analyzer (Malvern, UK).

HRTEM images were measured with a Tecnai G2 F20 field beam electron microscope (FEI Corp.) with an acceleration voltage of 200 kV. Elemental analysis was done by energy dispersive X-ray (EDX) spectra. The samples for HRTEM characterization were prepared by depositing $5\text{ }\mu\text{L}$ solution on a carbon-coated copper grid and drying at room temperature.

3. Results and discussion

3.1. Self-assembly of G-rich sequences

Our approach began with the design of G-rich oligonucleotide $\text{G}_2\text{T}_4\text{G}_4$ compared with the control sequences of $\text{G}_3\text{T}_4\text{G}_4$ and $\text{G}_4\text{T}_4\text{G}_4$. We analyzed the self-assembly structure of $\text{G}_2\text{T}_4\text{G}_4$, $\text{G}_3\text{T}_4\text{G}_4$ and $\text{G}_4\text{T}_4\text{G}_4$ in the presence of 100 mM Na^+ by CD, PAGE, AFM and SER spectra measurements. CD spectra of $\text{G}_4\text{T}_4\text{G}_4$ display the typical peak at 293 nm (Fig. 1a), suggesting the formation of dimeric antiparallel quadruplex structures involving four G-quartet planes [23], which show a fast mobility in the native PAGE images (Fig. 1b). When the number of guanine at 5' terminus of the sequence decreases from 4 to 3 and then to 2, the major peak at 293 nm still exists in CD spectra, but the melting temperature of the sequence decreases from 67.5 to $24\text{ }^{\circ}\text{C}$ and the electrophoresis mobility becomes slower (Fig. 1a and b). However, the relative low mobility band of $\text{G}_2\text{T}_4\text{G}_4$ is obviously faster than the 20 bp duplex marker. Combining with the previous work based on NMR studies [24,25], it is suggested that $\text{G}_3\text{T}_4\text{G}_4$ forms the dimmer antiparallel G-quadruplex with overhanging guanine residues, while $\text{G}_2\text{T}_4\text{G}_4$ forms the less compact antiparallel G-quadruplex with much more

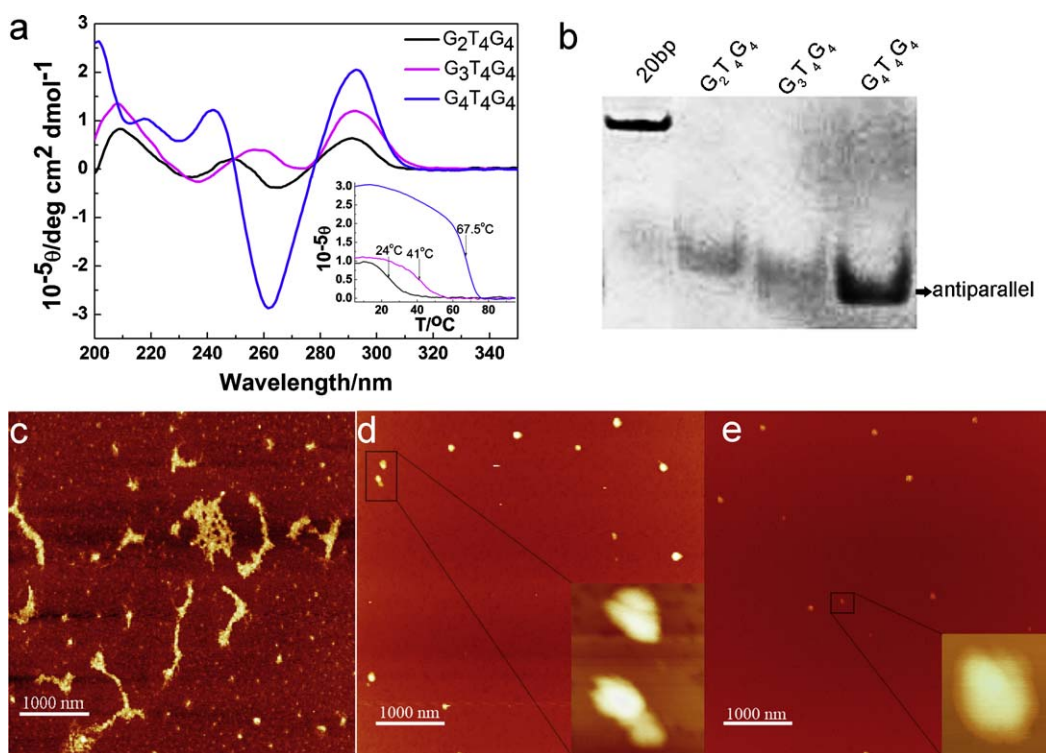


Fig. 1. (a) CD spectra of $\text{G}_2\text{T}_4\text{G}_4$, $\text{G}_3\text{T}_4\text{G}_4$, $\text{G}_4\text{T}_4\text{G}_4$ in 100 mM Na^+ solution (pH 5.9) at $20\text{ }^{\circ}\text{C}$. The inset indicates the CD melting curves of each DNA sequence. (b) Native PAGE images of $\text{G}_2\text{T}_4\text{G}_4$, $\text{G}_3\text{T}_4\text{G}_4$ and $\text{G}_4\text{T}_4\text{G}_4$ in 100 mM Na^+ solution (pH 5.9) at 10 V cm^{-1} and $4\text{ }^{\circ}\text{C}$. The first lane in the left is the 20 bp DNA marker. AFM images of self-assemblies of (c) $\text{G}_2\text{T}_4\text{G}_4$, (d) $\text{G}_3\text{T}_4\text{G}_4$, (e) $\text{G}_4\text{T}_4\text{G}_4$ in 100 mM Na^+ solution (pH 5.9).

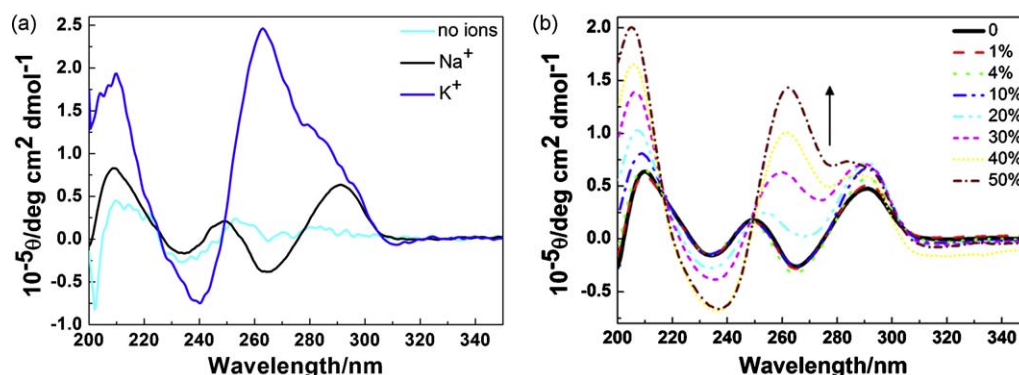


Fig. 2. (a) CD spectra of $G_2T_4G_4$ in the absence of ions, in the presence of 100 mM Na^+ and 100 mM K^+ (pH 5.9). (b) CD spectra of $G_2T_4G_4$ in 100 mM Na^+ at different ethanol content at 20 °C.

guanine residues overhung at the terminus. AFM images reflect the differences of the self-assembly structures of these three G-rich sequences. It is illustrated that $G_4T_4G_4$ only forms spheres with an average height of 2.0 nm (Fig. 1e), $G_3T_4G_4$ forms a few twin-sphere nanoparticles with an average height of 2.0 nm owing to the potential matches between overhanging guanines, while $G_2T_4G_4$ forms wire-like nanostructures with a height range of 0.6–1.4 nm (average height 1.0 ± 0.16 nm) and a length range of 0.3–1.7 μm together with small spheres in a height of 1.1 nm (Fig. 1c). These wire-like nanostructures of $G_2T_4G_4$ are attributed to base-pairings between the terminal overhanging guanines. SER spectra (Fig. 1S) display the structural similarity among $G_4T_4G_4$, $G_3T_4G_4$ and $G_2T_4G_4$, as well as a small peak shift around 1482 cm^{-1} , which will be discussed in the next section.

It is known that potassium ions are superior in stabilizing the G-quadruplex rather than sodium ions [26]. We compared conformational structures of $G_2T_4G_4$ in the presence of potassium ions with those in the presence of sodium ions. CD spectra of $G_2T_4G_4$ in 100 mM K^+ exhibit a strong positive peak around 263 nm and a shoulder around 293 nm, suggesting the formation of both the parallel and antiparallel G-quadruplex (Fig. 2a). As the potassium ions increased from 1 to 400 mM, native PAGE images display a fast mobility band corresponding to dimeric antiparallel G-quadruplexes and a slow band for four-stranded parallel G-quadruplexes (Fig. S2). AFM images of $G_2T_4G_4$ in 100 mM K^+ appear dispersed nanoparticles with the modal height around 1.1 and 2.5 nm, respectively (Fig. S3).

We further find that even in the presence of Na^+ the $G_2T_4G_4$ assembly structure can be modulated by the solvent content. With the increase of the ethanol content, CD spectra of $G_2T_4G_4$ in the presence of Na^+ gradually show the dominated peak at 265 nm corresponding to the parallel G-quadruplex [27] (Fig. 2b). The ethanol induced transition has two isoelliptic points at 249.5 and 216 nm, suggesting the existence of multi-state structural transition in the system, which is consistent with the appearance of the secondary melting temperature (T_m) in the CD melting curves as the ethanol concentration is higher than 40% (v/v) (Fig. S4). Similarly, Smirnov and Shafer have reported that addition of ethanol can stabilize the G-quadruplex of thrombin binding aptamer [28].

3.2. Self-organization of DNA-silica hybrid nanostructures

Upon adding APTMS ethanol solution into the aqueous solution, the hydrolysis reaction of this organosilane occurs immediately to form amino-coated silica nanoparticles [29], and the zeta potential of the silica nanoparticles synthesized without DNA was 2.5 mV at pH 5.9. When the aqueous solution contains

$G_2T_4G_4$, the zeta potential of silica nanoparticles turns to be -18 mV, illustrating the occurrence of interactions between amino-coated silica and $G_2T_4G_4$. Previous work also reported that amino-coated silica can interact with the negatively charged DNA molecules [7,30].

Fig. 3 shows significant variations of SER spectra and CD spectra of $G_2T_4G_4$ upon mixing with APTMS ethanol solution. SER spectra of $G_2T_4G_4$ display the typical peaks at 1238 cm^{-1} corresponding to the base dT, 1377 cm^{-1} for both dT and dG, 1324 and 1333 cm^{-1} reflecting the C2'-endo/syn dG and C2'-endo/anti dG conformation, as well as that at 1581 cm^{-1} indicating the hydrogen bonding of guanine involving exocyclic NH_2 donor sites [31–33]. It is worthwhile to mention that the peak at 1484 cm^{-1} is the indication of solvated guanine N7 site, while the peak at 1482 cm^{-1} indicates the Hoogsteen N7 hydrogen bonding of guanines [32]. As the number of 5' terminal guanine residues of $G_4T_4G_4$ reduces to 2, the peak shifts from 1482 to 1484 cm^{-1} (Fig. S1), indicating that the conformation of $G_2T_4G_4$ is not so same as the symmetric antiparallel G-quadruplex of $G_4T_4G_4$, especially there is less Hoogsteen base-pairings between guanine residues of $G_2T_4G_4$ molecules. Upon mixing with APTMS ethanol solution, the relative intensity of 1484 cm^{-1} is obviously enhanced, suggesting more solvated guanine N7 sites exist in the mixture of $G_2T_4G_4$ and silica.

CD spectra indicate diminishing of the typical G-quadruplex peak near 293 nm after mixing with APTMS ethanol solution, but the melting curve shows a transition temperature of $42\text{ }^\circ\text{C}$ with less cooperative, much higher than that of $G_2T_4G_4$. It is illustrated that as the hydrolysis reaction goes on the interactions between amino-coated silica and DNA make the unstable G-quadruplex of $G_2T_4G_4$ transform into a multi-stranded supermolecular structure. This structural transformation happens simultaneously with the hydrolysis reaction of APTMS, of which the observed rate constant is $k_{\text{obs } 293\text{ nm}} = 0.2479 \pm 0.0522\text{ s}^{-1}$ determined by CD stopped-flow experiments. In previous work, the dissociation rate constant of G-quadruplex resulted from mixing with its complementary sequence was in the magnitude order of 10^{-3} s^{-1} in the presence of sodium ions at $20\text{ }^\circ\text{C}$ [34].

DNA-silica hybrid nanostructures formed in 18 h hydrolysis reaction of APTMS were characterized by AFM images. As shown in Fig. 4, well-ordered leaf-vein nanostructures with regular interval branches were observed. It was clear that both patterned trunks and branches comprise of nanoparticles with average height of 55.5 ± 11.2 nm, and the interval between neighboring major branches is uniformly about $1.3 \pm 0.2\text{ }\mu\text{m}$. Such regularly branched DNA-silica nanostructures are quite different from the reported fractal-patterned dendritic nanostructures of metal nanoparticles [35,36] or polymers [37], grown under the mechanism of diffusion-

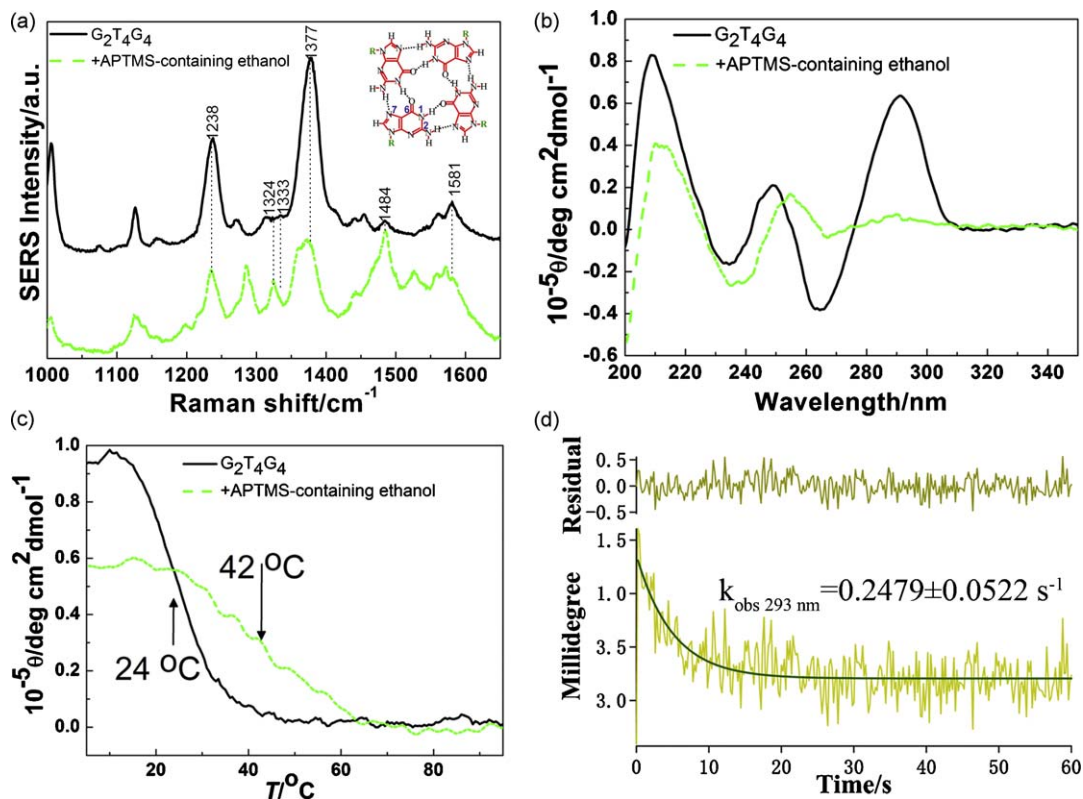


Fig. 3. (a) SER spectra, (b) CD spectra, and (c) CD melting curves of G₂T₄G₄ (100 mM Na⁺, pH 5.9) before and after mixing with APTMS ethanol solution. (d) Kinetic time course recorded at 293 nm upon mixing G₂T₄G₄ and APTMS-containing ethanol solution at 20 °C.

limited aggregate. Further, similar branched nanostructures were observed by HRTEM images (Fig. 5), which display the nanostructures consisting of nanoparticles with an average diameter of 38.0 ± 8.6 nm, surrounded by organic compounds, of which the intensity gradually decreases under the irradiation of electron beams. The EDX spectra (Fig. 5b) of the branched aggregates indicate the co-existence of element C, N, O, P, and Si, which are major components of DNA and

the hydrolysis products of APTMS. The construction difference of DNA-silica nanostructures between HRTEM and AFM images is attributed to the epitaxy and electriferous property of the mica against the copper grid of TEM [38,39]. In addition, in the absence of DNA, silica nanoparticles grow quickly to the modal size around 95 nm after 10 min hydrolysis reaction of APTMS (Fig. S5a) and continuously grow into large aggregates in 3 h hydrolysis reaction

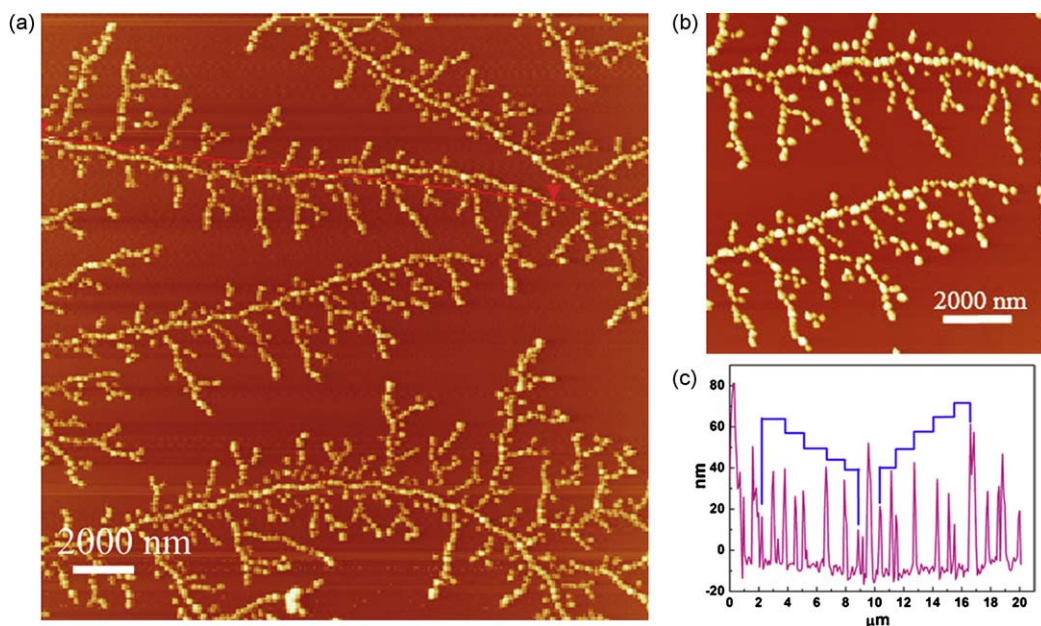


Fig. 4. (a) AFM images of leaf-vein nanostructures formed under the template of G₂T₄G₄ (100 mM Na⁺, pH 5.9). (b) An enlarged image of (a). (c) The height profile along the red line in (a), the blue ladder shows the interval of the branches. (For interpretation of the references to color in this figure legend, the reader is referred to the web version of the article.)

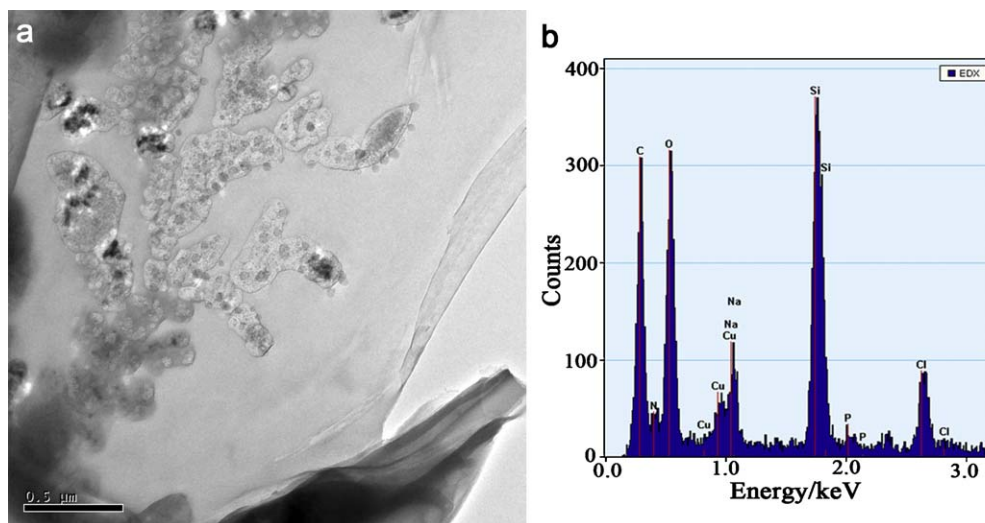


Fig. 5. (a) TEM images of branched $G_2T_4G_4$ -silica nanostructures in 100 mM Na^+ (pH 5.9). (b) Elemental composition of the nanostructures in (a) determined by EDX.

(Fig. S5b). Therefore, it is concluded that the interaction between $G_2T_4G_4$ and amino-coated silica results in the formation of the regularly branched nanostructures.

Moreover, we found that the DNA-silica nanostructures were sensitive to the conformational structure of DNA template. In the presence of 100 mM K^+ , $G_2T_4G_4$ mainly forms stable four-stranded parallel G-quadruplex with the melting temperature of 73 °C. Upon adding APTMS ethanol solution into the $G_2T_4G_4$ - K^+ aqueous solution, both CD and SER spectra (Fig. 6a and b) show few variations except that the melting temperature decreases from 73 to 60.5 °C, suggesting no structural transformation occurs for the four-stranded parallel G-quadruplex. Fig. 6c indicates the AFM image of the silica nanostructures formed in $G_2T_4G_4$ - K^+ solution, which were sphere particles with a height distribution around 4 and 6 nm (Fig. S6). In combination with the different self-assemblies of $G_2T_4G_4$ in the presence of Na^+ and K^+ ,

respectively, therefore it is concluded that the multi-stranded wire-like assemblies of $G_2T_4G_4$ in the presence of Na^+ play an important role in orienting the organization of leaf-vein silica nanostructures.

The ethanol content can also influence the DNA-silica hybrid structure. In the case of 40% (v/v) ethanol content, the melting curve of $G_2T_4G_4$ shows two transition temperature (39 and 54.5 °C), while the melting temperature of $G_2T_4G_4$ turns to be 46 °C after mixing with APTMS ethanol solution. The intensity of peaks at both 265 and 293 nm becomes lower in the CD spectra (Fig. 7a and b). Fig. 7c displays AFM images of similar branched DNA-silica nanostructures formed in 40% (v/v) ethanol solutions, with the average height of individual nanoparticle around 30 nm. Such smaller particle size is attributed to slower hydrolysis reaction rate of APTMS in high ethanol content solutions. The similarity of them demonstrated that multi-

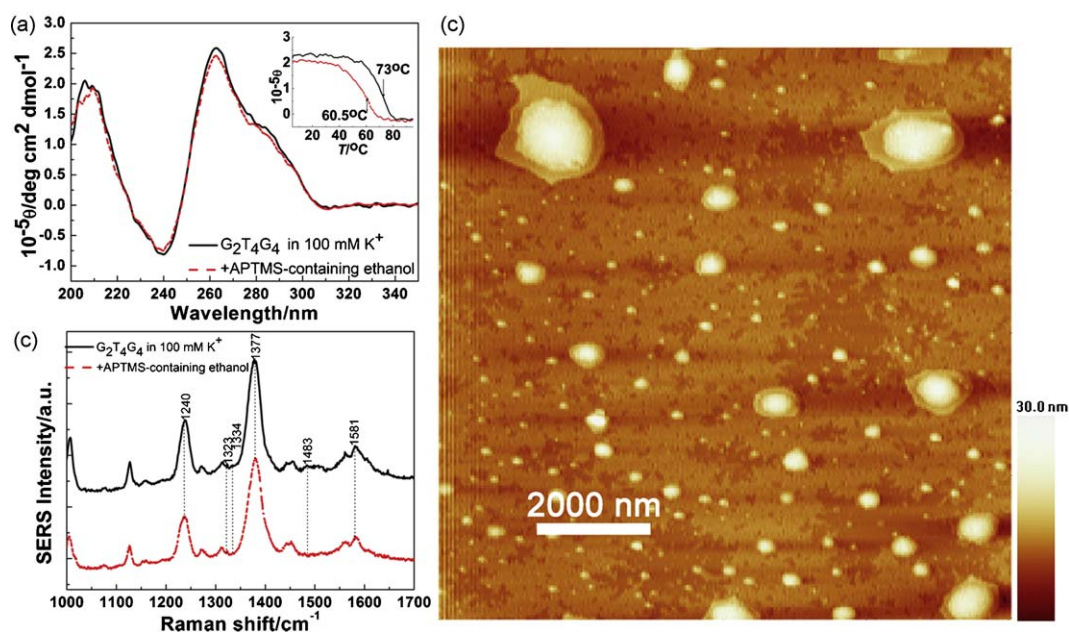


Fig. 6. (a) CD spectra and (b) SER spectra of $G_2T_4G_4$ (100 mM K^+ , pH 5.9) before and after mixing with APTMS ethanol solution at 20 °C. The inset: CD melting curves of $G_2T_4G_4$ in the above conditions. (c) AFM images of $G_2T_4G_4$ -silica nanostructures formed in the presence of 100 mM K^+ (pH 5.9).

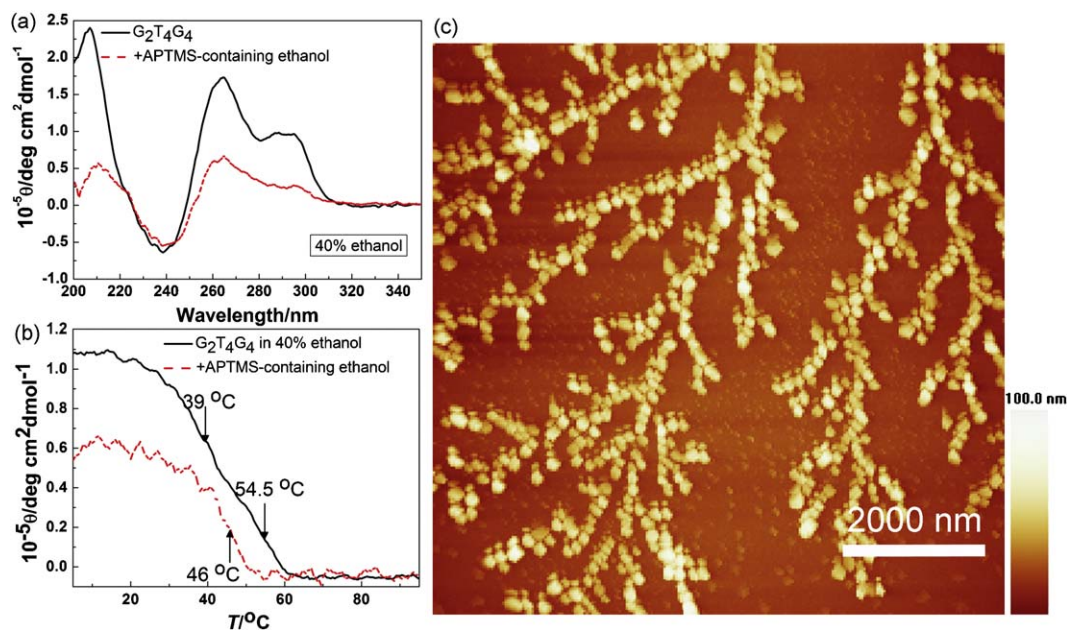


Fig. 7. (a) CD spectra and (b) CD melting curves of $G_2T_4G_4$ in 40% (v/v) ethanol solutions (100 mM Na^+ , pH 5.9) before and after mixing with APTMS ethanol solution at 20 °C. (c) AFM images of $G_2T_4G_4$ -silica nanostructures formed at the ethanol content of 40% (100 mM Na^+ , pH 5.9).

stranded supermolecular indeed induce the silica nanoparticles assembly.

4. Conclusions

We have demonstrated a novel approach to orient the organization of silica nanoparticles with leaf-vein branched nanostructures by using an original dynamic G-quadruplex transformation. Integrating the supermolecular assembly of DNA biomolecules with the hydrolysis process of organosilane, the branched silica nanostructures can be tuned through the cation species and the ethanol content. For the development of “bottom-up” nanobiotechnology, this original G-quadruplex transformation is a promising approach to generate programmable templates that can control the construction of regular branched nanostructures. Our work shows the capability for directing oxide nanoparticles into sophisticated nanoarchitectures, and this opens new avenues to construct regular branched nanostructures of semiconductor metal oxide nanoparticles for energy and catalysis applications.

Acknowledgements

This work was supported by the NSFC (nos. 20776102 and 20836005), the RFDP and the NCET.

Appendix A. Supplementary data

Supplementary data associated with this article can be found, in the online version, at doi:10.1016/j.materresbull.2010.08.008.

References

- [1] F.A. Aldaye, A.L. Palmer, H.F. Sleiman, *Science* 321 (2008) 1795–1799.
- [2] L. Berti, G.A. Burley, *Nat. Nanotechnol.* 3 (2008) 81–87.
- [3] Q. Gu, C.D. Cheng, R. Gonela, S. Suryanarayanan, S. Anabathula, K. Dai, D.T. Haynie, *Nanotechnology* 17 (2006) 14–25.
- [4] A. Houlton, A.R. Pike, M.A. Galindo, B.R. Horrocks, *Chem. Commun.* (14) (2009) 1797–1806.
- [5] Y. Lu, J.W. Liu, *Acc. Chem. Res.* 40 (2007) 315–323.
- [6] J. Sharma, R. Chhabra, A. Cheng, J. Brownell, Y. Liu, H. Yan, *Science* 323 (2009) 112–116.
- [7] C.Y. Jin, H.B. Qiu, L. Han, M.H. Shu, S.A. Che, *Chem. Commun.* (23) (2009) 3407–3409.
- [8] M. Numata, K. Sugiyasu, T. Hasegawa, S. Shinkai, *Angew. Chem. Int. Ed.* 43 (2004) 3279–3283.
- [9] S. Fujikawa, R. Takaki, T. Kunitake, *Langmuir* 21 (2005) 8899–8904.
- [10] J.M. Kinsella, A. Ivanisevic, *Langmuir* 23 (2007) 3886–3890.
- [11] K. Lund, Y. Liu, S. Lindsay, H. Yan, *J. Am. Chem. Soc.* 127 (2005) 17606–17607.
- [12] C. Sanchez, H. Arribart, M.M.G. Guille, *Nat. Mater.* 4 (2005) 277–288.
- [13] S. Burge, G.N. Parkinson, P. Hazel, A.K. Todd, S. Neidle, *Nucleic Acids Res.* 34 (2006) 5402–5415.
- [14] Y. Qin, L.H. Hurley, *Biochimie* 90 (2008) 1149–1171.
- [15] N. Sugimoto, *Bull. Chem. Soc. Jpn.* 82 (2009) 1–10.
- [16] T.C. Marsh, E. Henderson, *Biochemistry* 33 (1994) 10718–10724.
- [17] T.C. Marsh, J. Vesenska, E. Henderson, *Nucleic Acids Res.* 23 (1995) 696–700.
- [18] D. Miyoshi, H. Karimata, Z.M. Wang, K. Koumoto, N. Sugimoto, *J. Am. Chem. Soc.* 129 (2007) 5919–5925.
- [19] M.A. Batalia, E. Protozanova, R.B. Macgregor, D.A. Erie, *Nano Lett.* 2 (2002) 269–274.
- [20] E. Protozanova, R.B. Macgregor, *Biochemistry* 35 (1996) 16638–16645.
- [21] M. Biyani, K. Nishigaki, *Gene* 364 (2005) 130–138.
- [22] P.C. Lee, D. Meisel, *J. Phys. Chem.* 86 (1982) 3391–3395.
- [23] P. Schultze, F.W. Smith, J. Feigon, *Structure* 2 (1994) 221–233.
- [24] M. Crnugelj, P. Sket, J. Plavec, *J. Am. Chem. Soc.* 125 (2003) 7866–7871.
- [25] P. Sket, M. Crnugelj, J. Plavec, *Bioorg. Med. Chem.* 12 (2004) 5735–5744.
- [26] W. Li, P. Wu, T. Ohmichi, N. Sugimoto, *FEBS Lett.* 526 (2002) 77–81.
- [27] M. Vorlickova, K. Bednarova, I. Kejnovska, J. Kypr, *Biopolymers* 86 (2007) 1–10.
- [28] I.V. Smirnov, R.H. Shafer, *Biopolymers* 85 (2007) 91–101.
- [29] Y.G. Lee, J.H. Park, C. Oh, S.G. Oh, Y.C. Kim, *Langmuir* 23 (2007) 10875–10878.
- [30] D. Zhang, Y. Chen, H.Y. Chen, X.H. Xia, *Anal. Bioanal. Chem.* 379 (2004) 1025–1030.
- [31] L. Laporte, G.J. Thomas, *J. Mol. Biol.* 281 (1998) 261–270.
- [32] C. Krafft, J.M. Benevides, G.J. Thomas, *Nucleic Acids Res.* 30 (2002) 3981–3991.
- [33] T. Miura, G.J. Thomas, *Biochemistry* 34 (1995) 9645–9654.
- [34] W. Li, D. Miyoshi, S. Nakano, N. Sugimoto, *Biochemistry* 42 (2003) 11736–11744.
- [35] Y. Zhou, S.H. Yu, C.Y. Wang, X.G. Li, Y.R. Zhu, Z.Y. Chen, *Adv. Mater.* 11 (1999) 850–852.
- [36] L.B. Yang, B. Sun, F.L. Meng, M.Y. Zhang, X. Chen, M.Q. Li, J.H. Liu, *Mater. Res. Bull.* 44 (2009) 1270–1274.
- [37] H.Y. Gan, Y.L. Li, H.B. Liu, S. Wang, C.H. Li, M.J. Yuan, X.F. Liu, C.R. Wang, L. Jiang, D.B. Zhu, *Biomacromolecules* 8 (2007) 1723–1729.
- [38] M. Koepf, J.A. Wytko, J.P. Bucher, J. Weiss, *J. Am. Chem. Soc.* 130 (2008) 9994–10001.
- [39] J. Vesenska, D. Bagg, A. Wolff, A. Reichert, R. Moeller, W. Fritzsche, *Colloids Surf. B* 58 (2007) 256–263.